European Review for Medical and Pharmacological Sciences 2020; 24: 8210-8218

Analysis of clinical features and imaging signs of COVID-19 with the assistance of artificial intelligence

H.-W. REN[1], Y. WU[2], J.-H. DONG[1], W.-M. AN[1], T. YAN[3], Y. LIU[1], C.-C. LIU[1]

[1]Department of Radiology, Fifth Medical Center of Chinese PLA General Hospital, Beijing, P.R. China
[2]Qinghe Clinic, Northern Medical District of Chinese PLA General Hospital, Beijing, P.R. China
[3]International Liver Diseases Diagnosis and Treatment Center, Fifth Medical Center of Chinese PLA General Hospital, Beijing, P.R. China

Hongwei Ren and Yan Wu both contributed this manuscript equally

Abstract. – OBJECTIVE: To explore the CT imaging features/signs of patients with different clinical types of Coronavirus Disease 2019 (COVID-19) *via* the application of artificial intelligence (AI), thus improving the understanding of COVID-19.

PANTIENTS AND METHODS: Clinical data and chest CT imaging features of 58 patients confirmed with COVID-19 in the Fifth Medical Center of PLA General Hospital were retrospectively analyzed. According to the Guidelines on Novel Coronavirus-Infected Pneumonia Diagnosis and Treatment (Provisional 6th Edition), COVID-19 patients were divided into mild type (7), common type (34), severe type (7) and critical type (10 patients). The CT imaging features of the patients with different clinical types of COVID-19 types were analyzed, and the volume percentage of pneumonia lesions with respect to the lung lobes (where the lesion was located) and to the whole lung was calculated with the use of AI software. SPSS 21.0 software was used for statistical analysis.

RESULTS: Common clinical manifestations of COVID-19 patients: fever was found in 47 patients (81.0%), cough in 31 (53.4%) and weakness in 10 (17.2%). Laboratory examinations: normal or decreased white blood cell (WBC) counts were observed in 52 patients (89.7%), decreased lymphocyte counts (LCs) in 14 (24.1%) and increased C-reactive protein (CRP) levels in 18 (31.0%). CT imaging features: there were 48 patients (94.1%) with lesions distributed in both lungs and 46 patients (90.2%) had lesions most visible in the lower lungs; the primary manifestations in patients with common type COVID-19 were ground-glass opacities (GGOs) (23/34, 67.6%) or mixed type (17/34, 50.0%), with lesions mainly distributed in the periphery of the lungs (28/34, 82.4%); the primary manifestations of patients with severe/critical type COVID-19 were consolidations (13/17, 76.5%) or mixed type (14/17, 82.4%), with lesions distributed in both the peripheral and central areas of lungs (14/17,82.4%); other common signs, including pleural parallel signs, halo signs, vascular thickening signs, crazy-paving signs and air bronchogram signs, were visible in patients with different clinical types, and pleural effusion was found in 5 patients with severe/critical COVID-19. AI software was used to calculate the volume percentages of pneumonia lesions with respect to the lung lobes (where the lesion was located) and to the whole lung. There were significant differences in the volume percentages of pneumonia lesions for the superior lobe of the left lung, the inferior lobe of the left lung, the superior lobe of the right lung, the inferior lobe of the right lung and the whole lung among patients with different clinical types ($p<0.05$). The area under the ROC curve (AUC) of the volume percentage of pneumonia lesions for the whole lung for the diagnosis of severe/critical type COVID-19 was 0.740, with sensitivity and specificity of 91.2% and 58.8%, respectively.

CONCLUSIONS: The clinical and CT imaging features of COVID-19 patients were characteristic to a certain degree; thus, the clinical course and severity of COVID-19 could be evaluated with a combination of an analysis of clinical features and CT imaging features and assistant diagnosis by AI software.

Key Words:
Coronavirus Disease 2019, Computed tomography, Imaging features, Artificial intelligence.

Introduction

Coronavirus Disease 2019 (COVID-19), a disease caused by severe acute respiratory syndrome Coronavirus 2 (SARS-CoV-2), is mainly characterized by lung inflammatory lesions, and it has been reported that COVID-19 can also cause damage to the intestinal tract, liver and nervous system and produce corresponding symptoms[1-3]. Moreover,

Corresponding Author: Jinghui Dong, MD; e-mail: jpe637@163.com

SARS-CoV-2 is prone to large-scale spread as a result of the failure of timely detection and early isolation due to its long incubation time and strong infectiousness. According to the *Guidelines on Novel Coronavirus-Infected Pneumonia Diagnosis and Treatment* (Provisional 6th Edition) issued by the National Health Commission of the People's Republic of China[4], a comprehensive diagnosis should be carried out with the combination of epidemiology, clinical manifestations, and medical imaging and laboratory examinations in terms of the diagnostic criteria of COVID-19. Nucleic acid detection has been widely used in the diagnosis of COVID-19, but with a relatively high false-negative rate in the early stage of the disease, it may lead to delayed treatment of COVID-19 in some patients due to the failure of timely diagnosis, thus causing the spread of the virus. Interestingly, high-resolution CT (HRCT) examination has been suggested to play an important role in auxiliary diagnosis in the screening of COVID-19 patients, as it can be easily and rapidly performed and yields high-resolution images[5]. This study aimed to investigate the clinical and CT imaging features of patients with different clinical types of COVID-19 and to provide important reference values for clinical diagnosis and treatment with the assistance of artificial intelligence (AI)-based quantitative analysis.

Patients and Methods

General Information

The clinical data of 58 patients confirmed with COVID-19 in the Fifth Medical Center of PLA General Hospital were collected. All confirmed cases met the diagnostic criteria of the *Guidelines on Novel Coronavirus-Infected Pneumonia Diagnosis and Treatment* (trial version sixth)[4]. Among the 58 COVID-19 patients, there were 30 males and 28 females aged 15-85 years old, with a mean age of 49.1±16.9 years. Based on the COVID-19 clinical classification, there were 7 patients with mild type, 34 with common type, 7 with severe type and 10 with critical type.

Epidemiological History and Clinical Data

Of the 58 patients, 55 had a clear history of close contact with epidemic areas and infected people, and 3 had unclear causes of disease. The clinical data were retrospectively analyzed, mainly consisting of clinical symptoms and signs (fever, cough, weakness, etc.) and laboratory examinations [white blood cell (WBC) count, lymphocyte count (LC) and C-reactive protein (CRP) level)].

Methods

CT examination: A Lightspeed VCT 64-slice CT scanner (GE Medical Systems, USA) was used. Patients underwent CT examination in a head-first supine position, entering the scanner in a breath-holding manner. The scanning range was from the apex of the lung to the level of the bilateral costophrenic angles. Scanning parameters: tube voltage, 120 kV; auto-milliampere technique, 40-250 mA; noise index (NI) = 25; pitch, 0.984:1; matrix, 512 × 512; and slice thickness, 5 mm. Lung window settings: window width/level, 2000/-600 HU; mediastinal window, 350/40 HU, axial reconstruction of lung window, slice thickness, 0.625 mm.

CT image analysis: the images were read independently by two experienced radiologists. When there was a disagreement, a consensus was finally obtained by consultation between the two radiologists. In this study, the CT manifestations of patients were mainly described according to the following features: (1) shape and distribution of the lesions; (2) location of the lesions; (3) general signs of the lesions: ground glass opacities (GGOs), consolidation shadows, fibroses, etc.; (4) other common signs: crazy-paving signs, pleural parallel signs, air bronchogram signs, vascular thickening signs, halo signs and reversed halo signs; (5) extrapulmonary manifestations: the presence or absence of pleural effusions; and (6) the volume percentage of pneumonia lesions with respect to the whole lung: quantitative calculation was performed by using Biomind COVID-19 edition AI software (Beijing Andeyizhi Technology Co., Ltd. Beijing, China). The AI software could specifically identify the lung algorithm sequence for 1-5 mm slice thicknesses/slice spacings in the DICOM data of the chest CT plain scan images. The AI model automatically segmented the lung inflammatory lesions and the regions of interest (ROIs) of each lung lobe in the chest CT images of the patient. Calculations were carried out based on the spatial relation of the segmentation results and the related volume pixel values, and the localization information of each single lesion and the quantitative information (volume and lesion/lobe volume ratio) were output. For the sum of all the lesions, the volume ratio of all the lesions with respect to the whole lung was calculated, as well as the density distribution curve (all lesions, lung).

Statistical Analysis

All data were analyzed by SPSS 21.0 statistical software (IBM Corp., Armonk, NY, USA). Qualitative data are expressed as frequencies and

ratios, and quantitative data are expressed as x ± s for normal distributions and medians (interquartile range) for non-normal distributions. The chi-squared test or Fisher's exact probability test was applied to the comparisons of the CT imaging signs among the different clinical types. For the volume percentage of pneumonia lesions with respect to the whole lung for the different clinical types, data from each set were subjected to a test of normality. For data with normal distributions, one-way ANOVA was applied, and comparisons between groups were performed by least-significant difference (LSD) for data with homogeneity of variance or Tamhane's method for data without homogeneity of variance; for data with a non-normal distribution, the Kruskal-Wallis test was used, and the Mann-Whitney U test was used for comparisons between groups. $p<0.05$ was considered statistically significant.

Results

Clinical Manifestations of COVID-19 Patients

The 58 COVID-19 patients had different clinical symptoms, mainly including fever in 47 patients (81.0%), cough in 31 (53.4%) and weakness in 10 (17.2%). Laboratory examinations showed that there were 52 patients (89.7%) with normal or decreased WBC count, 14 (24.1%) with decreased LC and 18 (31.0%) with increased CRP level. The main clinical features and laboratory examinations of COVID-19 patients with different clinical types are shown in Table I.

CT Imaging Features of COVID-19 Patients

Distribution of lesion locations (Table II)

There were 3 patients (5.9%) with involvement in the right lung only and 48 patients (94.1%) with involvement in both lungs. There were 40 patients (78.4%) with involvement in the superior lobe of the right lung, 31 (60.8%) with involvement in the middle lobe of the right lung, 46 (90.2%) with involvement in the inferior lobe of the right lung, 40 (78.4%) with involvement in the superior lobe of the left lung and 44 (86.3%) with involvement in the inferior lobe of the left lung.

Common signs (distribution and shape) (Table III)

1) GGO shadows, consolidation shadows and cord-like shadows, mainly distributed in subpleural regions (Figure 1A). 2) Large patch shadows, with a wide distribution of lesions, or fusion into a large area (diffuse distribution), thereby resulting in the formation of a white lung.

Other Common Signs

1) Pleural parallel signs (Figure 1B and 2B): subpleural band shadows parallel to the pleura.

Table I. Main clinical symptoms and laboratory examinations of COVID-19 patients (No., %).

Clinical types	No. (%)	Fever	Cough	Weakness	Normal/ decreased WBC count	Decreased LC	Increased CRP level
Mild type	7 (12.1)	5 (71.4)	3 (42.9)	1 (14.3)	7 (100)	1 (14.3)	2 (28.6)
Common type	34 (58.6)	27 (79.4)	15 (44.1)	2 (5.9)	32 (90.9)	5 (14.7)	8 (23.5)
Sever type	7 (12.1)	6 (85.7)	6 (85.7)	3 (42.9)	5 (71.4)	3 (42.9)	3 (42.9)
Critical type	10 (17.2)	9 (90.0)	7 (70.0)	4 (40.0)	8 (80.0)	5 (50.0)	5 (50.0)

Note: COVID-19, Coronavirus Disease 2019; WBC, white blood cell; LC, lymphocyte count; CRP, C-reactive protein.

Table II. Distribution of lung lesion locations of COVID-19 patients (%).

Lung lobe/ segment	Superior lobe of right lung	Middle lobe of right lung	Inferior lobe of right lung	Superior lobe of left lung	Inferior lobe of left lung	Both lungs	Right lung only	Left lung only
No.	40	31	46	40	44	48	**3**	0
Percentage (%)	78.4	60.8	90.2	78.4	86.3	94.1	**5.9**	0

Note: COVID-19, Coronavirus Disease 2019.

Table III. CT manifestations of 51 cases with common and severe/critical type COVID-19 [n(%)].

CT signs	Common type (n = 34)	Severe/critical type (n = 17)	χ^2	*P*
Lesion distribution location				
Peripheral involvement	28 (82.4)	13 (76.5)		0.714
Peripheral and central involvement	15 (44.1)	14 (82.4)	6.755	0.009
Lesion shape				
Ground glass opacity	23 (67.6)	12 (70.6)	0.046	0.831
Consolidation	8 (23.5)	13 (76.5)	13.114	0.000
Mixed type	17 (50.0)	14 (82.4)	4.977	0.026
Other common signs				
Pleural parallel sign	8 (23.5)	6 (35.3)		0.336
Halo sign	10 (29.4)	5 (29.4)	0.000	1.000
Vascular thickening sign	12 (35.3)	10 (58.9)	2.558	0.110
Fine reticular opacity (crazy-paving sign)	9 (26.5)	6 (35.3)	0.425	0.514
Air bronchogram sign	17 (51.5)	10 (55.6)	0.354	0.552
Pleural effussion	2 (6.1)	5 (27.8)	_	0.034

Note: COVID-19, Coronavirus Disease 2019.

2) Halo signs: ground-glass-like changes around consolidation lesions (Figure 1C). 3) Vascular thickening signs: clear signs of blood vessels passing through the lesions in sub-consolidation

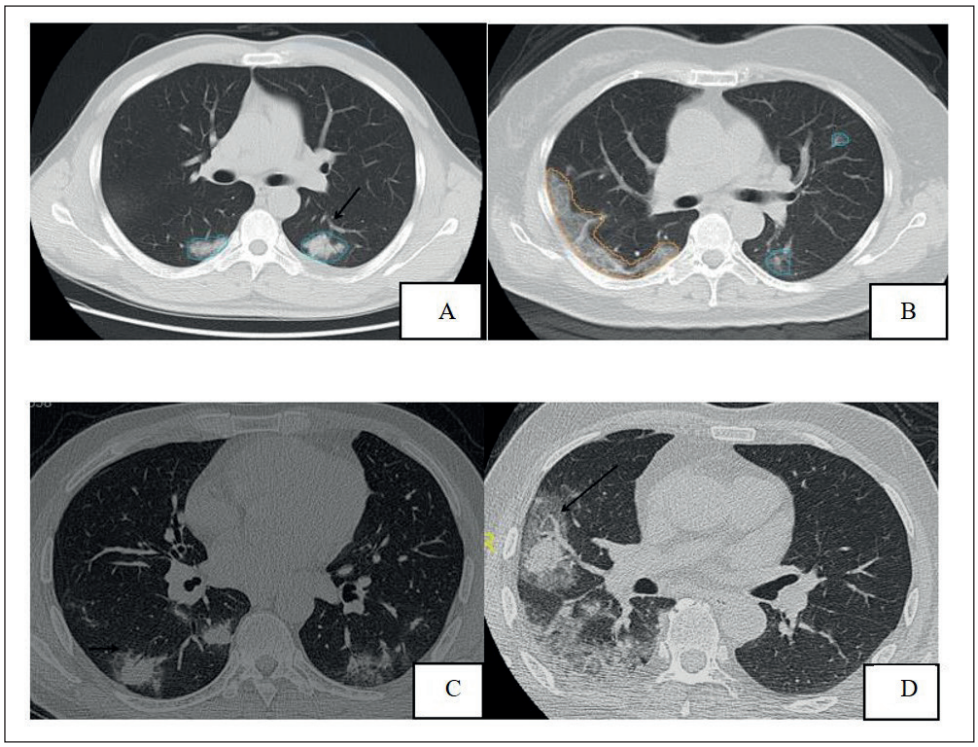

Figure 1. A, COVID-19 patient (common type): male, 37 years old. Bilateral subpleural patch-like high-density shadows were found, with visible air bronchogram signs in the left lesions (arrow). **B,** COVID-19 patient (normal type): female, 53 years old. Band-shaped, high-density shadows and small patch-like high-density shadows were found in the bilateral subpleural regions, with the presence of ground glass-like changes, and some lesions were parallel to the pleura. The volume percentage of pneumonia lesions with respect to the whole lung was 10.51%. **C,** COVID-19 patient (severe type): male, 48 years old. Multiple patchy and nodular consolidations were visible in the subpleural regions of the inferior lobes of both lungs, and halo sign changes (arrow) andair bronchogram signs were observed in some of the lesions. **D,** A COVID-19 patient (severe type): male, 48 years old. Multiple patchy high-density shadows were found in the inferior lobe of the right lung, wherein a nodular shadow indicated the presence of halo sign changes in the periphery, and a vascular thickening shadow was found in the lesion (arrow).

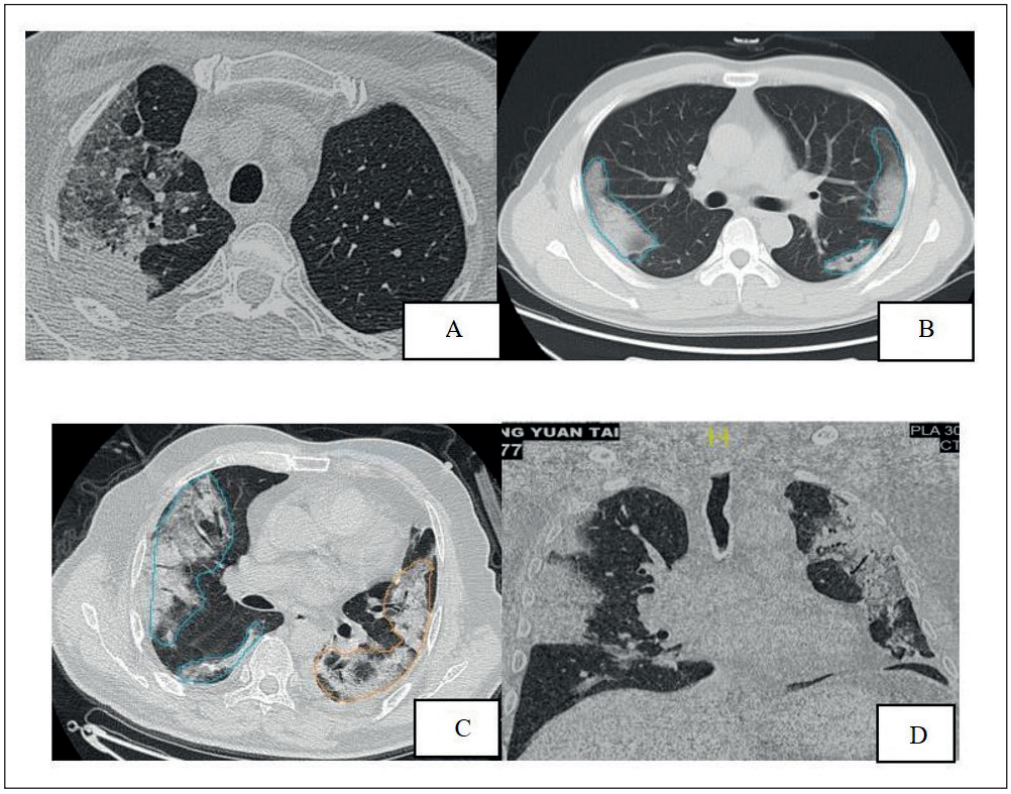

Figure 2. A, COVID-19 patient (critical type), male, 78 years old. In the apical segment of the superior lobe of the right lung, a patchy high-density shadow was found, with visibile partial consolidations and local crazy-paving sign changes. **B**, COVID-19 patient (critical type), male, 34 years old. A banded-shaped high-density shadow was found in the subpleural regions of the bilateral superior lobes, parallel to the pleura. **C-D**, COVID-19 patient (critical type), male, 74 years old. There were multiple patchy high-density shadows in both lungs, with the presence of partial consolidation; most of the lesions were located in the subpleural regions, with a visible air bronchogram sign inside. The volume percentage of pneumonia lesions with respect to the whole lung was 27.59%.

lesions, and visible diameter thickening in some blood vessels (Figure 1D). 4) Fine reticular opacity or crazy-paving signs: interlobular and intralobular septum thickening (Figure 2A). 5) Air bronchogram signs: contrast formed between the consolidation of lung tissues and the air-containing bronchus, with visibility of blood vessels normally passing through the lesions and unobstructed lumen (Figure 2C and 2D).

Extrapulmonary Manifestations

There were 7 patients with pleural effusion, including 2 with the common type of COVID-19, 2 with the severe type and 3 with the critical type. Quantitative analysis of the volume proportions of lesions by AI (Table IV): the volume percentages of pneumonia lesions with respect to the lung lobes (lesion located) and the volume percentages of all lesions with respect to the whole lung: further comparisons in the volume percentages of the lesions with respect to the superior lobe of left lung, the inferior lobe of left lung, the superior lobe of right lung and the inferior lobe of right lung between patients with different clinical types of the disease were carried out, and the results showed that there were significant differences in the volume percentages of pneumonia lesions with respect to the inferior lobe of the right lung and the volume percentage of all pneumonia lesions with respect to the whole lung between patients with the common type and the critical type of the disease ($p<0.05$). In addition, the volume percentages of the pneumonia lesions in patients with common type COVID-19 were significantly lower than those in patients with severe type COVID-19 ($p<0.001$) and in patients with critical type COVID-19 ($p<0.002$), and the volume percentages of the pneumonia lesions in patients with severe type COVID-19 were also sig-

Table IV. Volume percentages of lung lesions with respect to different lesion locations in patients with different clinical types of COVID-19 [%, median (interquartile range)].

Lesion location	Common type (n = 34)	Severe type (n = 7)	Critical type (n = 10)	Z	P
Superior lobe of left lung	0.29 (0.03~1.89)	0.40 (0~14.63)	6.46 (0.91~8.82)	5.955	0.051
Inferior lobe of left lung	3.24 (1.38~8.15)	2.72 (0.57~14.88)	20.43 (4.59~49.97)	6.105	0.047
Superior lobe of right lung	0.26 (0.04~3.07)	2.42 (0.39~13.17)	12.21 (3.93~20.70)	14.806	0.001
Middle lobe of right lung	0.01 (0.0~3.14)	0.20 (0.0~7.06)	3.99 (0.18~10.31)	3.059	0.217
Inferior lobe of right lung	4.29 (0.39~14.93)	7.77 (4.06~26.77)	15.64 (6.0~35.56)	6.088	0.048
Whole lung	3.25 (0.39~5.76)	4.63 (2.21~15.82)	13.11 (4.05~25.04)	8.478	0.014

Note: COVID-19, Coronavirus Disease 2019.

nificantly lower than those in patients with critical type COVID-19 (p= 0.030). The ROC curve of the volume percentage of the pneumonia lesions with respect to the whole lung generated to predict the diagnosis of patients with severe type and critical type COVID-19 is shown in Figure 3. With a cut-off value of 9.88%, the area under the ROC curve (AUC) was 0.740, with a sensitivity and specificity of 91.2% and 58.8%, respectively, indicating high diagnostic efficacy. Specifically, when the percentage of pneumonia lesion volume to the whole lung volume was ≥ 9.88%, patients were diagnosed with severe type COVID-19 or critical type COVID-19. When the percentage of pneumonia lesion volume to the whole lung volume was <9.88%, patients were diagnosed with common type COVID-19.

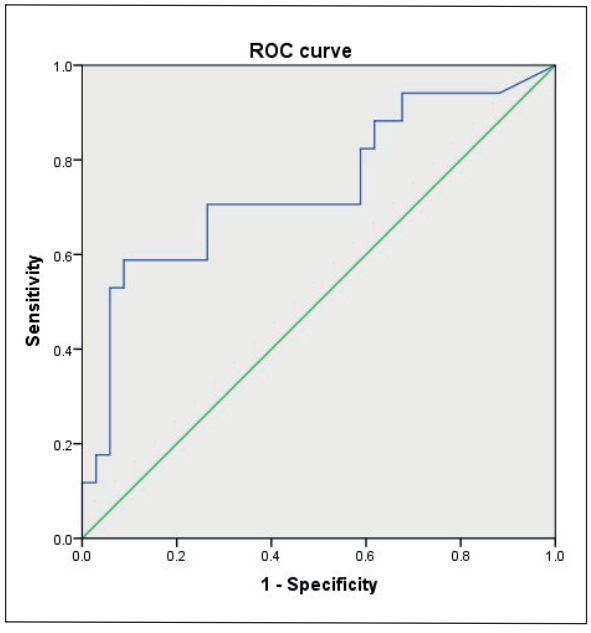

Figure 3. ROC curve of the volume percentage of the pneumonia lesion with respect to the whole lung in the differential diagnosis of severe type and critical type COVID-19 patients.

Discussion

Nucleic acid detection has been suggested as the gold standard for the diagnosis of COVID-19 according to the updated diagnosis and treatment guidelines issued by the National Health Commission of the People's Republic of China. However, preliminary data and reports from several designated hospitals in Wuhan and throughout China have indicated that nucleic acid detection shows a certain hysteretic nature and degree of false negativity[6]. HRCT is very sensitive in the detection of lesions and can perform this detection before the presentation of clinical symptoms and even earlier than the nucleic acid test. Therefore, the important roles of HRCT in preclinical screening, early diagnosis and evaluation of treatment effects should be emphasized.

Clinical Manifestations

It has been reported that the most common symptoms in COVID-19 patients are fever and cough[7-8]. In our study, there were in 47 patients (81.0%) with fever as the initial symptom and 31 (53.4%) with cough. In terms of laboratory examinations, COVID-19 patients mainly manifested the hemogram characteristics of viral infection; 52 patients (89.7%) had normal or decreased peripheral WBC counts, 14 (24.1%) had decreased LCs and 18 (31.0%) had increased CRP levels.

Preliminary Analysis of CT Imaging Features of COVID-19

CT imaging features of COVID-19 patients in the early stage: round-like GGO changes were more likely to be observed, and the location of the lesions was relatively limited, mainly distributed in the subpleural regions, which may be related to the infection mode of the viral pneumonia, namely, respiratory droplet transmission.

COVID-19 is caused by a SARS-CoV-2 infection with small particles, and SARS-CoV-2 causes bronchiolitis and peripheral inflammation after inhalation through the airway, spreading to the furthest end and invading the lung tissues, thus involving the lung interstitium[9]. Therefore, regarding the imaging features, lesions in COVID-19 patients in the early stage manifested with GGOs and were mostly located in the subpleural regions, which may be related to the pathological mechanism of the infection; in the early stage of the viral pneumonia, the lung parenchyma around the terminal and respiratory bronchioles may be involved, followed by spread of the involvement to the whole lung lobules, resulting in diffuse alveolar damage[10].

With the progression of the course of the disease, the number of lesions gradually increased, and expanded ranges were found; the lesions then spread to the entire secondary lobule. The main CT manifestations of severe and critical COVID-19 patients included multiple patchy, mixed high-density shadows in both lungs, consolidations for some lesions and coexistence of GGO and consolidation shadows, and a diffuse distribution of lesions in the entire lung lobe was observed in a few critical type COVID-19 patients, with the possible presence of white lung. Pleural effusion was found in 5 patients with critical type COVID-19 in the study, suggesting that pleural effusion may be a sign of severe pneumonia[11].

Other common signs of COVID-19 were found: 1. Fine reticular opacities (crazy-paving signs), with pathological changes including interlobular and intralobular septum thickening, reflecting the presence of interstitial lesions and viral invasion of the intralobular interstitium. 2. Pleura parallel signs: lesions manifested as subpleural band shadows, with the long axis of the lesion parallel to the pleura, which is mainly caused by the lymphatic return in the peripheral regions of the lung lobules and drainage towards the peripheries of subpleural regions and interlobular septa[12]. The lesions were first involved in the cortex and lung tissues, without conforming to the lung segment anatomical distribution, which is important in the differentiation of the lesion distribution to that in bacterial pneumonia[13]. 3. Air bronchogram signs: there was normal passing-through regarding the air-bearing bronchus in consolidated lung tissues without thickening. The virus was mainly involved in the peripheral interstitium and had little effect on the bronchus, with no necrosis, little mucus and little bronchial blockage. In addition, there was no evident central interstitial thickening or bronchial thickening. 4. Vascular thickening signs and thickening of blood vessels were found in the lesions, which was consistent with the general process of inflammation. It was thought that due to inflammatory stimulation, vascular permeability increased, blood capillaries expanded, and the corresponding pulmonary artery thickened. 5. Halo signs and reserved halo signs: the halo sign is presumed to indicate infiltration of the lesions (mainly in the lobules and central nodules) into the peripheral interstitium, that is, the image formed by the aggregation of interstitial inflammatory cells. The reserved *halo sign* was shown as a GGO shadow in the center, with the periphery completely or almost completely surrounded by a high-density shadow. The presence of the reserved halo sign in COVID-19 may indicate inflammatory repair mainly on the edges, resulting in the formation of band shadows tending to consolidate on the edges, while the central repair was relatively delayed.

AI has been well applied in the rapid screening of diseases and in performing accurate and quantitative diagnoses. AI has also been initially applied in the diagnosis of COVID-19. In our study, BioMind COVID-19 version AI software was applied to rapidly identify and analyze chest CT images. Intelligent segmentation of the lesion areas and quantitative calculation of the volume percentages of the pneumonia lesions with respect to the lung lobes (where the lesions were located) and the percentage of the whole pneumonia lesion volume to the whole lung volume were carried out so that the progression of the disease could be objectively evaluated. We found that there were significant differences in the percentage of the whole pneumonia lesion volume to the whole lung volume among patients with common type COVID-19, patients with severe type COVID-19 and patients with critical type COVID-19, with an increasing tendency of the volume percentages of lesions with severity, which was consistent with the results of Lu et al[14] concerning a study on the correlation between CT imaging signs and clinical manifestations in COVID-19 patients with different clinical types. Therefore, the combination of clinical and CT imaging features and AI was conducive to the evaluation of the severity of the disease and could also provide accurate and quantitative evaluation indicators for the progression of the disease, which can be beneficial for assessing the dynamic evaluation of the lesions. With respect to the CT images in the

COVID-19 patients in our study, all segments of the lung lobes were involved, especially in the inferior lobes of both lungs. Specifically, there were 46 patients (90.2%) with involvement in the inferior lobe of the right lung (more visible), which is consistent with the results of a previous imaging study on H7N9 avian influenza[15]. A possible explanation of the findings may be that the inferior lobes and peripheral pulmonary lobules were well developed, wherein the blood capillary, lymphatic vessels, interstitial cells and matrix were very dominant. The reason for the greater visibility of multiple involvement in the inferior lobe of right lung may be related to the fact that the primary bronchi in this lobe were relatively short, steep and straight in terms of traveling direction[16], providing the virus an easier path to entry.

Conclusions

The clinical manifestations of COVID-19 mainly included fever, cough, weakness, etc., and COVID-19 patients had characteristic CT imaging manifestations. The combination of quantitative data analysis with the use of AI software and nucleic acid detection can be conducive to the clinical diagnosis and treatment of COVID-19. There were still some deficiencies in this study, such as the small sample size, short follow-up time, and unclear changes in image manifestations and lung function after patients were discharged from the hospital; thus, further studies are still needed to conduct a more in-depth analysis.

Authors' Contributions

Hongwei Ren, Yan Wu, Jinghui Dong: conceived and designed the experiments; Weimin An, Tao Yan: performed the experiments; Yuan Liu, Changchun Liu: analysis and interpretation of the experimental results. All the authors have read and approved the final version of the manuscript and agreed to be accountable for all aspects of the work.

Ethical Approval

The study was approved by the Institutional Ethics Committee of The Fifth Medical Center of Chinese PLA General Hospital, and written informed consent was obtained from all participants.

Conflict of Interests

The authors declare that there are no conflicts of interest.

References

1) Phan LT, Nguyen TV, Luong QC, Nguyen TV, Nguyen HT, Le HQ, Nguyen TT, Cao TM, Pham QD. Importation and human-to-human transmission of a Novel Coronavirus in Vietnam. N Engl J Med 2020; 382: 872-874.
2) Groot RJ, Baker SC, Baric RS, Brown CS, Drosten C, Enjuanes L, Fouchier RA, Galiano M, Gorbalenya AE, Memish ZA, Perlman S, Poon LL, Snijder EJ, Stephens GM, Woo PC, Zaki AM, Zambon M, Ziebuhr J. Middle East Respiratory Syndrome Coronavirus (MERS-CoV): announcement of the Coronavirus Study Group. J Virol2013; 87: 7790-7792.
3) Chau TN, Lee KC, Yao H, Tsang TY, Chow TC, Yeung YC, Choi KW, Tso YK, Lau T, Lai ST, Lai CL. SARS-associated viral hepatitis caused by a novel coronavirus: report of three cases. Hepatology, 2004, 39: 302-310.
4) Guidelines on the Novel Coronavirus-Infected Pneumonia Diagnosis and Treatment (Provisional 6th Edition). Available at: http://www.nhc.gov.cn/yzygj/s7653p/202002/8334a8326dd94d329df351d7da8aefc2.shtml.
5) Ksiazek TG, Erdman D, Goldsmith CS, Zaki SR, Peret T, Emery S, Tong S, Urbani C, Comer JA, Lim W, Rollin PE, Dowell SF, Ling AE, Humphrey CD, Shieh WJ, Guarner J, Paddock CD, Rota P, Fields B, DeRisi J, Yang JY, Cox N, Hughes JM, LeDuc JW, Bellini WJ, Anderson LJ; SARS Working Group. A Novel Coronavirus associated with Severe Acute Respiratory Syndrome. N Engl J Med 2003; 348: 1953-1966.
6) Zhang N, Wang L, Deng X, Liang R, Su M, He C, Hu L, Su Y, Ren J, Yu F, Du L, Jiang S. Recent advances in the detection of respiratory virus infection in humans. J Med Virol 2020; 92: 408-417.
7) Huang C, Wang Y, Li X, Ren L, Zhao J, Hu Y, Zhang L, Fan G, Xu J, Gu X, Cheng Z, Yu T, Xia J, Wei Y, Wu W, Xie X, Yin W, Li H, Liu M, Xiao Y, Gao H, Guo L, Xie J, Wang G, Jiang R, Gao Z, Jin Q, Wang J, Cao B. Clinical features of patients infected with 2019 Novel Coronavirus in Wuhan, China. Lancet 2020; 395: 497-506.
8) Li Q, Guan X, Wu P, Wang X, Zhou L, Tong Y, Ren R, Leung KSM, Lau EHY, Wong JY, Xing X, Xiang N, Wu Y, Li C, Chen Q, Li D, Liu T, Zhao J, Liu M, Tu W, Chen C, Jin L, Yang R, Wang Q, Zhou S, Wang R, Liu H, Luo Y, Liu Y, Shao G, Li H, Tao Z, Yang Y, Deng Z, Liu B, Ma Z, Zhang Y, Shi G, Lam TTY, Wu JT, Gao GF, Cowling BJ, Yang B, Leung GM, Feng Z. Early transmission dynamics in Wuhan, China, of novel coronavirus-infected pneumonia. N Engl J Med 2020; 382: 1199-1207.
9) Hwang DM, Chamberlain DW, Poutanen SM, Low DE, Asa SL, Butany J. Pulmonary pathology of severe acute respiratory syndrome in Toronto. Mod Pathol 2005; 18 : 1-10.
10) Worthy SA, Müller NL, Hartman TE, Swensen SJ, Padley SP, Hansell DM. Mosaic attenuation pattern on thin-section CT scans of the lung: differentiation among infiltrative lung, airway, and

vascular diseases as a cause. Radiology 1997; 205: 465-470.

11) Jin YH, Cai L, Cheng ZS, Cheng H, Deng T, Fan YP, Fang C, Huang D, Huang LQ, Huang Q, Han Y, Hu B, Hu F, Li BH, Li YR, Liang K, Lin LK, Luo LS, Ma J, Ma LL, Peng ZY, Pan YB, Pan ZY, Ren XQ, Sun HM, Wang Y, Wang YY, Weng H, Wei CJ, Wu DF, Xia J, Xiong Y, Xu HB, Yao XM, Yuan YF, Ye TS, Zhang XC, Zhang YW, Zhang YG, Zhang HM, Zhao Y, Zhao MJ, Zi H, Zeng XT, Wang YY, Wang XH; for the Zhongnan Hospital of Wuhan University Novel Coronavirus Management and Research Team, Evidence-Based Medicine Chapter of China International Exchange and Promotive Association for Medical and Health Care (CPAM). A rapid advice guideline for the diagnosis and treatment of 2019 Novel Coronavirus (2019-nCoVSARS-CoV-2) infected pneumonia (standard version). Mil Med Res 2020; 7: 4.

12) Lei J, Li J, Li X, Qi X. CT Imaging of the 2019 novel coronavirus severe acute respiratory syndrome coronavirus 2 (2019-nCoVSARS-CoV-2) pneumonia. Radiology 2020; 295: 18.

13) Li P, Zhang JF, Xia XD, Su DJ, Liu BL, Zhao DL, Liu Y, Zhao DH. Serial evaluation of high-resolution CT findings in patients with pneumonia in novel swine-origin influenza A (H1N1) virus infection. Br J Radiol 2012; 85: 729-735.

14) Huang L, Han R, Yu PX, Wang SK, Xia LM. Study on correlation between CT features and clinical manifestations in patients with different clinical types of novel coronavirus pneumonia. Chin J Radiol 2020; 54: E003.C.

15) Chen ZL Liu D, Wang JJ, Shen HL. Clinic presentations and imaging features of a novel avian-origin influenza H7N9%. J Pract Radiol 2015; 31: 1560-1562.

16) Kim EA, Lee KS, Primack SL, Yoon HK, Byun HS, Kim TS, Suh GY, Kwon OJ, Han J. Viral pneumonias in adults: radiologic and pathologic findings. Radiographics 2002; 22 Spec No: S137-S149.